Distinct forms of cholinergic modulation in parallel thalamic sensory pathways

D. M. Mooney*, L. Zhang*, C. Basile*, V. V. Senatorov†, J. Ngsee*, A. Omar*, and B. Hu*‡§

*Ottawa Health Research Institute and University of Ottawa, Ottawa, ON, Canada K1Y 4E9; ‡Department of Clinical Neurosciences, Faculty of Medicine, University of Calgary, Calgary, AB, Canada T2N 4N1; and †National Institute of Mental Health, National Institutes of Health, Bethesda, MD 20892-1272

Edited by Rodolfo R. Llinas, New York University Medical Center, New York, NY, and approved October 24, 2003 (received for review July 16, 2003)

Mammalian thalamus is a critical site where early perception of sensorimotor signals is dynamically regulated by acetylcholine in a behavioral state-dependent manner. In this study, we examined how synaptic transmission is modulated by acetylcholine in auditory thalamus where sensory relay neurons form parallel lemniscal and nonlemniscal pathways. The former mediates tonotopic relay of acoustic signals, whereas the latter is involved in detecting and transmitting auditory cues of behavioral relevance. We report here that activation of cholinergic muscarinic receptors had opposite membrane effects on these parallel synaptic pathways. In lemniscal neurons, muscarine induced a sustained membrane depolarization and tonic firing by closing a linear K^+ conductance. In contrast, in nonlemniscal neurons, muscarine evoked a membrane hyperpolarization by opening a voltage-independent K^+ conductance. Depending on the level of membrane hyperpolarization and the strength of local synaptic input, nonlemniscal neurons were either suppressed or selectively engaged in detecting and transmitting synchronized synaptic input by firing a high-frequency spike burst. Immunohistochemical and Western blotting experiments showed that nonlemniscal neurons predominantly expressed M2 muscarinic receptors, whereas lemniscal cells had a significantly higher level of M1 receptors. Our data indicate that cholinergic modulation in the thalamus is pathway-specific. Enhanced cholinergic tone during behavioral arousal or attention may render synaptic transmission in nonlemniscal thalamus highly sensitive to the context of local synaptic activities.

Parallel synaptic signaling is a highly conserved neural computational mechanism in the mammalian thalamocortical system. Across virtually every sensory modality, ascending pathways from the thalamus are subdivided into two systems known as the lemniscal (primary) and nonlemniscal (associative) projections. A large number of studies have shown that primary and associative neurons differ in many ways in their anatomical connections, mode of sensory response, and physiological roles in sensory perception (1–4). For example, in the medial geniculate body (MGB) of auditory thalamus, lemniscal, and nonlemniscal neurons are separated into a ventral core (MGv) and a surrounding belt that occupies entire caudodorsal pole (MGd) of the MGB (5, 6). The former pathway mediates high fidelity relay of auditory afferents to the primary auditory cortex whereas the latter is involved in transmitting behaviorally significant sensory cues directly to the lateral amygdala and many areas of association auditory cortices, temporal lobe, and parahippocampal limbic structures (6–12). Acquired auditory cues, but not neutral sounds, lead to brisk and high frequency neuronal firing in nonlemniscal neurons (4). Such a parallel organization of auditory-sensing pathways renders the thalamus an important site for facilitating sensory perception and integration. Indeed, MGd neurons and other $Calbindin_{D28k}$-positive neurons in the thalamus are thought to form a matrix system that may, via their diffuse cortical projections, play an important role in thalamocortical synchronization (6).

The cellular basis of parallel synaptic sensing and information processing presents an important, yet poorly defined, physiological issue. Recent *in vitro* studies suggest that lemniscal and nonlemniscal neurons may possess different intrinsic membrane properties. Thus, nonlemniscal cells of the auditory thalamus are more hyperpolarized than their ventral counterparts (13, 14). They tend to discharge a burst of spikes in response to an excitatory postsynaptic potential (EPSP) that is coupled to a low threshold Ca^{2+} spike (LTS) (13, 15). The bias toward burst firing in matrix neurons points to an appealing synaptic communication mechanism because bursting not only enhances the strength and reliability of synaptic transmission (16, 17), but may also provide a robust trigger for eliciting persistent cortical excitation or cortical dysrhythmia (18, 19). The mode of synaptic responses in the thalamus is, however, not solely determined by intrinsic membrane properties but rather is dynamically regulated by brainstem cholinergic input, which by releasing ACh and activating muscarinic receptors alters neuronal membrane potential and firing pattern in a behavioral state dependent manner (20, 21). Presently, little is known about how the parallel auditory pathways are modulated by ACh, despite their striking differences in connectivity and functional properties (9). To address this important issue, we recorded muscarinic membrane current and synaptic responses from rat MGB neurons maintained *in vitro*. We report here that muscarine had opposite effects on lemniscal and nonlemniscal cells: it depolarized the former but hyperpolarized the latter. As a result of this differential cholinergic modulation, MGv and MGd can be engaged into distinct modes of synaptic information processing.

Methods

Preparations, Electrophysiological Recording, and Data Analysis. The preparation of MGB explants and slices (22) followed Ottawa Hospital Animal Care Committee-approved protocols. Male Long-Evans rats (200–300 g) were decapitated, and the left half of the brain was isolated and pinned to the Sylgard base of a humidified recording chamber (School of Pharmacy, University of London, London). The temporal-occipital lobes and hippocampal tissues adjacent to the MGB were aspirated to expose the free surfaces of the MGB, which was superfused with oxygenated (95% O_2/5% CO_2), warmed (32–34°C) artificial cerebrospinal fluid at 4–6 ml/min. The artificial cerebrospinal fluid had a final pH of 7.6 and an osmolality of 295 ± 2 mOsM/kg, and contained 122 mM NaCl, 3 mM KCl, 1.3 mM $MgCl_2$, 25.9 mM $NaHCO_3$, 3.0 mM $CaCl_2$, and 11 mM glucose. For preparing coronal MGB slices, tissue blocks from Long-Evans rats (70–150 g) were cut on a vibrotome (300 μm) and incubated in artificial cerebrospinal fluid for 1–2 h before usage (14).

Both intracellular and whole-cell recording techniques were used in the present study. The latter was primarily done in MGB slices because slicing significantly increased the yield of stably

This paper was submitted directly (Track II) to the PNAS office.

Abbreviations: ACh, acetylcholine; MGB, medial geniculate body; DG, dentate gyrus; BIC, brachium of the inferior colliculus; LTS, low threshold Ca^{2+} spike; EPSP, excitatory postsynaptic potential; MGv, ventral nucleus of the MGB; MGd, caudodorsal nucleus of the MGB; CP, cerebral peduncle.

§To whom correspondence should be addressed. E-mail: hub@ucalgary.ca.

© 2003 by The National Academy of Sciences of the USA

www.pnas.org/cgi/doi/10.1073/pnas.0304445101

patched neurons. Intracellular recording electrodes were filled with 4 M potassium acetate and 0.15 M KCl, whereas the patch electrode solution (pH 7.4) contained 130 mM potassium gluconate, 10 mM NaCl, 10 mM KCl, 10 mM Na-Hepes, 1 mM EGTA, and 4 mM Mg-ATP. All electrophysiological experiments were performed at 34°C. Signals were conventionally amplified by using Axoclamp-2A or Axopatch amplifiers (Axon Instruments, Foster City, CA) and digitized at 22 kHz. During whole-cell recording, up to 80% of the series resistance was compensated. The liquid junction potential was subtracted online. All data are expressed as mean ± SEM.

The thalamic explants retain two visible and separate axonal projections to the MGB: ascending sensory afferents from the brachium of the inferior colliculus (BIC) and descending corticothalamic input coursing within the cerebral peduncle (CP). Our recordings were restricted to the ventral portion of MGB and its caudodorsal tip, of which the latter sends substantial projections to lateral amygdala, paralimbic, and association auditory cortices (8, 11). Synchronized or compound EPSPs were evoked by a bipolar-stimulating electrode inserted into the BIC and/or CP 1–2 mm from the MGB. For inducing randomly occurring EPSPs, we applied 4-aminopyridine (0.5 mM), either locally into the BIC through a micropipette (tip = 10 μm) or by bath solution. We purchased ACh, 4-aminopyridine, (+)-muscarine, and pirenzepine from Research Biochemicals (Natick, MA) and the rest of the drugs from Sigma. All antagonists were bath-applied. Agonists were steadily infused into the artificial cerebrospinal fluid by a timer-controlled syringe pump to produce the final concentration indicated in the text (23). Carbachol was always applied in the presence of 0.1 mM hexamethonium to block a transient nicotinic response, which occurred occasionally in some cells.

Immunohistochemistry, Western Blot, and RT-PCR. The immunohistochemistry was performed as described (14). Frontal sections (40 μm) were incubated in normal goat serum (4%) together with 0.3% Triton X and 0.05% Tween 20 (Sigma) and thereafter with rabbit anti-M1 or anti-M2 receptor affinity-purified polyclonal Abs (Chemicon) as recommended by the supplier. The secondary Ab, an Alexa Fluor 488 goat anti-rabbit IgG (H+L) conjugate (Molecular Probes) diluted 1:100 in 0.1 M PBS, was used to detect anti-M1 and anti-M2 Abs in separate sections. We performed positive control experiments in the hippocampal dentate gyrus (DG; Fig. 2*d*) where immunofluorescence-labelings (DG-IF) of muscarinic receptors were found overlapping with granule cells counterstained with Hoechst 33342 (Molecular Probes) (24). For M1 and M2 immunofluorescent detection, sections were mounted on an epifluorescence microscope equipped with a CCD camera and a frame grabber. They were excited at 495 nm with emission at 519 nm. Counterstaining was visualized by excitation at 350 nm with emission at 461 nm. Areas of MGv and MGd (Fig. 2*c*) from randomly selected sections ($n = 36$ each) were captured at a magnification of ×20 and printed out on grid square paper with proper coding. The number of fluorescent dots or puncta within a constant area was first counted manually by an examiner blinded to the intervention and later verified by computerized density measurements by using NORTHERN ECLIPSE software (Empix, Mississauga, ON, Canada). The densities of fluorescent puncta were compared between MGv and MGd regions by using Student's *t* tests. Data are expressed as mean ± SEM.

For Western blotting, dorsal and ventral tissue samples were taken from MGB explants ($n = 30$). Membranes from the supernatant were collected by centrifugation, and protein concentration was determined by Bradford assay (Bio-Rad). The protein samples (50 μg) were separated on SDS/PAGE and subjected to Western analysis by using M1 and M2 receptor Abs (Chemicon). Horseradish peroxidase-labeled secondary Abs and enhanced chemiluminescence were used to detect the bound primary Abs. The band intensities were quantified by densitometric analysis. For RT-PCR, total RNAs were isolated from MGv and MGd by using the RNeasy Mini Kit (Qiagen), and cDNAs were generated with RETROscript (Ambion, Austin, TX). PCR amplification was carried out by using oligonucleotide primers specific to M1, M2, and actin for 25–40 cycles in 5-cycle increments. The resulting PCR products were fractionated in 2% agarose gel and stained with ethidium bromide. Band intensities were quantified by densitometry.

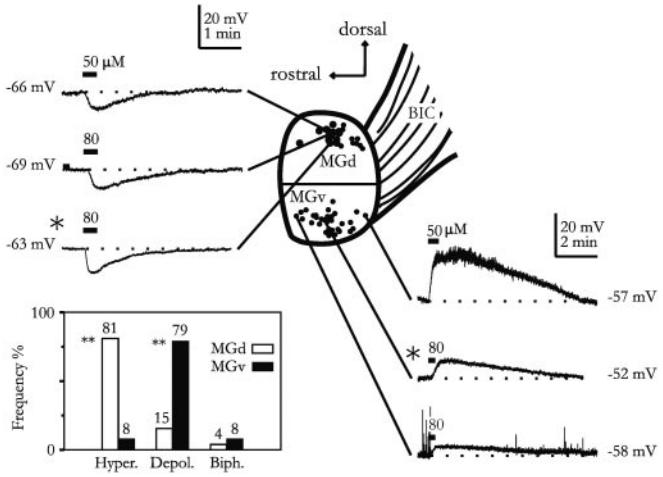

Fig. 1. Contrasting muscarinic responses in MGd and MGv neurons. Intracellular recordings of muscarinic responses obtained from the MGB explant are shown. Recording positions of individual neurons from different explants are indicated by the black dots. *, Recordings from same explant. (*Inset*) Percentage of different response types observed in MGd and MGv. Hyper, hyperpolarization; Depol, depolarization; Biph, biphasic response (hyperpolarization followed by depolarization). **, $P < 0.001$.

Results

The database of this study consisted of 106 MBG neurons that showed reproducible membrane responses to muscarinic agonists. Of these neurons, 43 were from MGv and the rest were from MGd. As shown in Fig. 1, we found that neurons recorded from MGv and MGd in thalamic explants clearly exhibited distinct muscarinic responses. Bath applications of muscarine (50–80 μM; 20 s) or carbachol (0.5 mM; 30 s) to MGd neurons resulted primarily in a membrane hyperpolarization (5.2 ± 0.5 mV; $n = 27$) lasting 160 ± 10 s ($n = 16$). By contrast, similar drug application in MGv neurons led to a membrane depolarization (7.7 ± 0.7 mV; $n = 15$) that was significantly longer than the MGd response (390 ± 40 s; $n = 20$; $P < 0.01$). Only a small number (<2%) of neurons in rat MGB showed biphasic responses. The opposite membrane responses of MGv and MGd cells can be obtained in the same explant (Fig. 1), and both muscarinic hyperpolarization and depolarization persisted after blockade of local synaptic transmission by tetrodotoxin (0.3–1.0 μM; $n = 9$). Furthermore, the hyperpolarizations were reversibly suppressed by tropicamide or atropine (50 μM; $n = 3$). At low agonist concentrations (10–20 μM), pirenzepine (1 μM) completely blocked the depolarization response but was only partially effective against hyperpolarization ($n = 5$), suggesting involvement of M1 receptors in muscarinic depolarization. To further examine the underlying receptor mechanism, we immunohistochemically stained MGv and MGd sections by using Abs against M1 and M2 receptors. Overall, rat MGB showed light M1 and M2 receptor staining. Under high magnification, fluorescent signals mainly appeared, in both MGB and DG, as dots or puncta (Fig. 2 *a* and *d*), many of which may derive from dendritic

NEUROSCIENCE

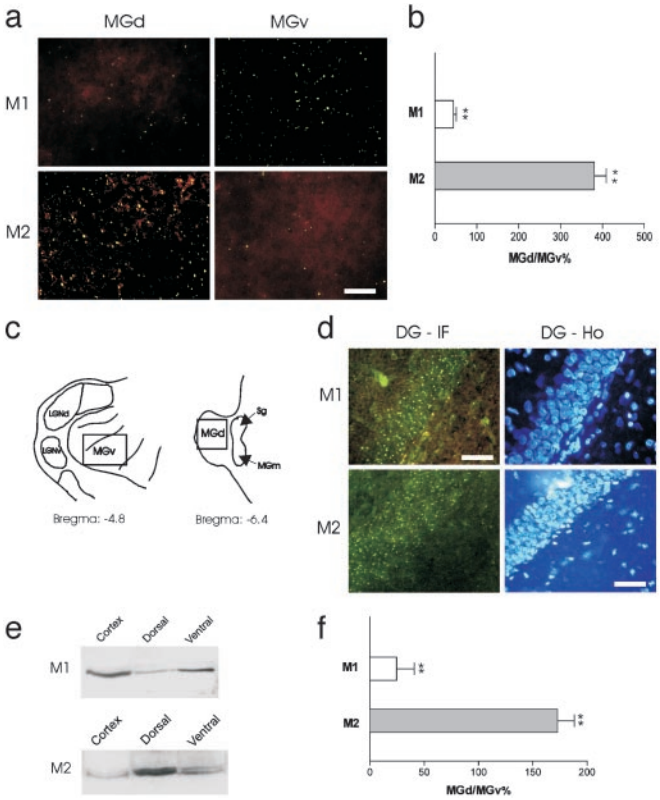

Fig. 2. Differential expression of muscarinic receptors. (*a*) Representative micrographs of M1 and M2 receptor labeling obtained from the same MGB. (*b*) Differential distribution of M1 and M2 receptors in MGd and MGv. The data are expressed as the percentage of total puncta obtained from MGd divided by that from MGv. (*c*) The approximate MGB locations of tissue sections used for immunoquantifications. (*d*) Positive controls in the hippocampal DG. Immunofluorescence labeling (DG-IF) of muscarinic receptors was found overlapping with Hoechst counterstained granule cells (DG-Ho) in the same sections. (*e*) Western blotting gels showing different levels of M1 (68 kDa) and M2 (73/75 kDa) receptors obtained from MGv and MGd. Cortical tissues were used as the positive control. (*f*) Difference in M1 and M2 receptor proteins between MGd and MGv. The data are expressed as in *b*.

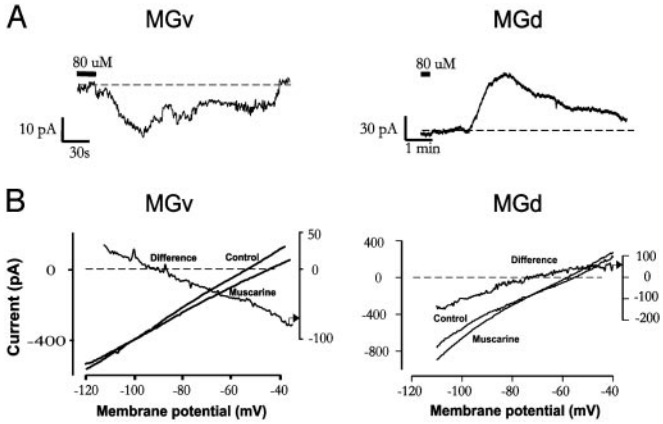

Fig. 3. Muscarine-evoked membrane currents in MGd and MGv neurons. (*A*) Examples of whole-cell voltage-clamp recordings of muscarinic responses obtained from MGd and MGv slices. (*B*) Representative I–V relationships of muscarinic currents. Slow voltage ramps were applied during control and in the presence of muscarinic agonist. Net muscarinic or ''Difference'' current was obtained by subtraction of the control I–V from the muscarinic I–V. Note the linearity of both inward and outward currents.

staining (25, 26). As illustrated in Fig. 2, the density of fluorescent puncta of M2 receptors in MGd was found to be significantly higher (≈3-fold) than that in MGv ($P < 0.001$). In contrast, M1 receptors displayed an opposite interregional difference ($P < 0.001$; Fig. 2 *a–d*). Differential expression of M1 and M2 receptors in MGd and MGv was also uncovered with Western blotting, albeit at a more moderate level (Fig. 2 *e* and *f*). We also performed RT-PCR experiments for M1 and M2 receptors cDNAs by using RNAs extracted from MGd cells. When normalized to the actin mRNA, the level of M2 mRNA in MGd is approximately twice that of M1 receptor mRNA (MGd/MGv = 2.07 ± 0.29; $n = 3$).

Whole-cell muscarinic membrane currents were recorded under voltage clamp. As reported (14), MGv and MGd neurons exhibited different levels of resting membrane potential (−65 ± 1.1 mV vs. −69.9 ± 1.5 mV; $P < 0.01$). Application of muscarinic agonists induced an inward current in MGv (I_{MGv}; $n = 12$) but an outward current in MGd (I_{MGd}; $n = 16$; Fig. 3*A*). The amplitudes of I_{MGv} and I_{MGd} measured at −60 mV were 60.54 ± 17 pA ($n = 9$) and 74.11 ± 11 pA ($n = 10$), respectively. Slow voltage ramps (3 mV/s) were used to clamp membrane voltage before and during drug application (Fig. 3*B*). Muscarinic current derived from subtraction of two ramp currents displayed two types of I–V relationships: crossing (89% of cases) and parallel (11% of cases). I_{MGv} was associated with a linear decrease (27.6 ± 4.48%) in slope conductance whereas I_{MGd} exhibited a linear increase (20.5 ± 5.2%) in slope conductance. The reversal potentials for I_{MGv} and I_{MGd} were −82.04 ± 6.4 mV and −92.68 ± 3.8 mV, respectively. Because the calculated equilibrium potential for K^+ in our experiments was −98 mV, I_{MGv} and I_{MGd} were likely mediated by a closing or opening of a voltage-independent K^+ conductance.

It is known that membrane hyperpolarization in thalamic neurons prompts intrinsic burst firing through deinactivation of LTS or through EPSP–LTS coupling (13, 15, 27). To examine how synaptic transmission is modulated during muscarinic hyperpolarization in MGd, we recorded synaptic potentials evoked by ascending sensory (BIC) and/or descending corticothalamic pathway stimulation. One such example is shown in Fig. 4, in which BIC and corticothalamic afferents were costimulated at 10 and 5 Hz with the cell held at −53 or −73 mV, respectively. We found that muscarinic modulation of nonlemniscal neurons is not unimodal. It inhibited tonic synaptic firing if evoked from a holding membrane potential above −60 mV (Fig. 4*A*) but induced strong burst responses from a more negative holding potential (Fig. 4*B*). The synaptic burst discharge occurred exclusively during muscarinic hyperpolarization and only followed the EPSPs coelicited from synchronized BIC and corticothalamic stimuli (Fig. 4*B*). Apparently, such a membrane condition can be used by nonlemniscal cells to selectively detect and transmit synchronized or strong synaptic events but suppress weaker ones. To analyze this unconventional synaptic mechanism in a more physiological context, we examined the mode of synaptic firing in MGd neurons triggered by random, continuous EPSPs of varying amplitudes (as opposed to artificially synchronized EPSPs evoked by electrical shocks). As illustrated in Fig. 5 *a* and *b*, LTS bursts, characterized by a short duration (15 ± 1 ms; $n = 30$) and high frequency (218 ± 9 Hz; $n = 30$) spike discharge, could be elicited by spontaneous EPSPs or by their summation with the EPSP evoked by a single shock applied to BIC afferents (Fig. 5*b*). EPSP–LTS coupling occurred within a narrow voltage window (−64 to −77 mV; Fig. 5 *b* and *c*) during muscarinic hyperpolarization and was invariably triggered by large synaptic potentials (10 ± 0.4 mV; Fig. 5*c*), most of which are temporally grouped or clustered within the 100 ms immediately preceding a burst (Fig. 5*d*). Smaller and isolated synaptic potentials (4.7 ± 0.3 mV) did not fire the neuron during the

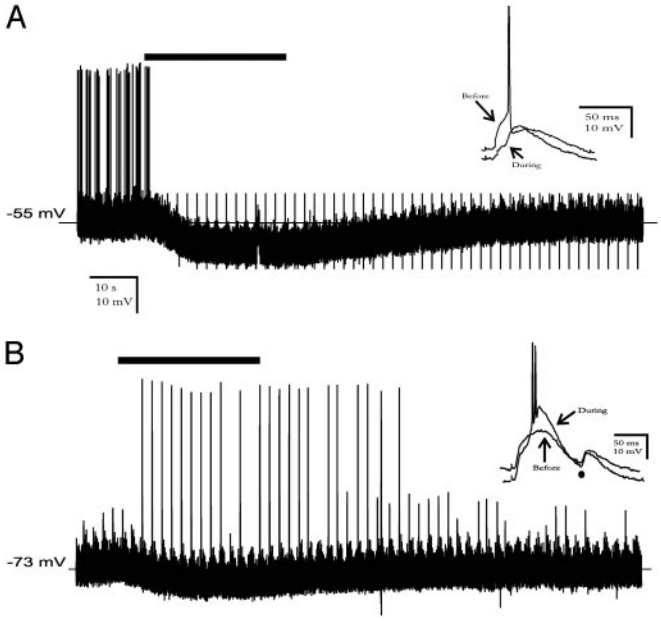

Fig. 4. Membrane potential dependence of muscarinic modulation of synaptic firing in MGd cells. (*A*) Intracellular recordings from a representative MGd cell showing that muscarine (50 μM, bar), when applied at a more depolarized level, inhibited synaptic firing evoked by costimulation of CP and BIC afferents. CP and BIC stimuli were delivered continuously at 10 Hz and 4.76 Hz, respectively. The synchronization of the two stimuli occurred every 2 s. (*Inset*) EPSPs and spiking evoked by simultaneous CP and BIC stimuli were suppressed during muscarinic hyperpolarization. (*B*) Synaptic firing recorded from the same neuron from a more negative membrane potential set by DC current injection. Notice that synaptic firing was triggered only during muscarinic hyperpolarization and by simultaneous CP and BIC stimuli (*Inset*). Smaller EPSPs evoked by single-pathway (•) stimulation were ineffective in firing the cell.

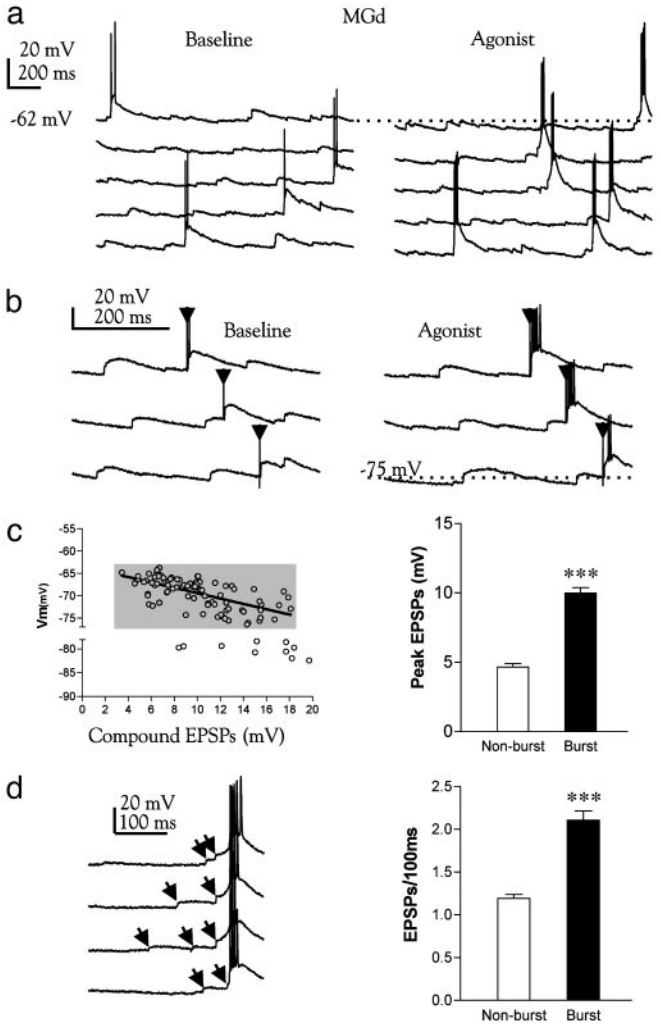

Fig. 5. Detection of synchronized synaptic events in MGd neurons by burst firing and muscarinic hyperpolarization. (*a*) Expanded consecutive recordings from a representative MGd neuron, separated by offsets for clarity. The spontaneous EPSPs trigger only one or two spikes at low frequency before muscarine application. A small muscarinic hyperpolarization (dotted line) causes EPSPs to trigger a high-frequency burst. (*b*) Burst firing is preferentially mediated by large EPSPs or EPSP summation. Traces are consecutive recordings. Arrowheads indicate stimulus artifacts. (*c Left*) The amplitude of burst-inducing EPSPs at different membrane voltages. Approximately 89% of all EPSP-burst complexes (gray box) can be best fit by a regression line (slope = -0.60 ± 0.08; $P < 0.0001$). (*Right*) The mean amplitudes of burst-inducing and nonbursting EPSPs. (*d*) Expanded recordings showing burst firing is triggered by temporally clustered EPSPs (arrows). The EPSP frequency occurring within a 100-ms time window immediately preceding a burst is significantly higher than the EPSPs frequency occurring in 100-ms windows not followed by burst events (*Right*). Data were pooled from three neurons (burst events, 44; nonburst events, 100; ***, $P < 0.0001$).

hyperpolarization. In contrast, lemniscal cells responded to spontaneous synaptic input with a single spike and tonic discharge during muscarinic application (data not shown), consistent with previous reports (23, 28). These results indicate that during muscarinic hyperpolarization, nonlemniscal neurons may become selectively sensitive to temporally correlated synaptic inputs and able to detect and amplify such synaptic events by generating a spike burst.

Discussion

In this study, we have investigated the membrane and synaptic responses of rat MGB neurons after muscarinic receptor activation. Our data demonstrate a significantly different pattern of muscarinic responses and receptor expression in lemniscal and nonlemniscal auditory thalamus. As a result, synaptic transmission in the MGB is differentially influenced by ACh in a pathway-specific manner. We propose that ACh serves as a highly selective neuromodulator that actively facilitates, rather than diminishes, parallel sensory processing in the sensory thalamus.

Our data confirm previous studies in rat and cat that muscarinic receptor activation produces a sustained membrane depolarization and tonic firing in lemniscal thalamocortical relay neurons (23, 28–30). Indeed, very few lemniscal neurons fire in burst *in vivo* in responding to sensory stimuli (31–33). The depolarization membrane response is primarily mediated by the closing of voltage-independent leak K^+ conductance as evidenced by the lack of rectification of muscarinic current and its insensitivity to Ca^{2+}-dependent K^+ channel blockade (unpublished observation). In a subset of neurons, the muscarinic current displayed a parallel I–V relationship with no apparent reversal potential. This type of response may derive from a concurrent inhibition and activation effect of muscarine on resting K^+ channels and an inward nonselective cation conductance, which may cancel out the net membrane resistance change (30, 34, 35). Whether this mixed action of muscarine may also partially contribute to the more positive reversal potential of muscarinic current in MGv, which expresses a significantly higher level of a hyperpolarization-activated nonselective cation conductance than the MGd cells (13), requires further study.

One of the main findings of our study is that an overwhelming majority of neurons located in the nonlemniscal portion of the

MGB are hyperpolarized by muscarine. Muscarinic hyperpolarization has been described in GABAergic reticular nucleus (21, 36), GABAergic interneurons of the lateral geniculate nucleus (37), and certain neurons from the cat and guinea pig MGB (28). Whether the hyperpolarizing neurons from these latter two species belong to nonlemniscal nuclei requires further investigation. Our data demonstrate that cholinergic modulation in the auditory thalamus is organized in a synaptic pathway-specific fashion. Such a parallel organization of cholinergic modulation is consistent with the notion that lemniscal and nonlemniscal MGB represent two largely independent sensory channels. Besides anatomical segregation, nonlemniscal nuclei differ in many aspects from their lemniscal counterparts (9). For example, MGd exhibits significantly higher level of *N*-methyl-D-aspartate receptors (38), strong staining by calbindin$_{D\text{-}28K}$ (6), and, in bats, selective 2-DG uptake during flying (39). The differential expression of muscarinic receptors reported here further suggests lemniscal and nonlemniscal neurons are endowed with different neuromodulatory signaling mechanisms. Mammalian thalamus predominantly expresses M1 and M2 receptors (25, 30, 40). In rat lateral geniculate nucleus, immunohistochemical work confirmed the presence of M3 receptors (41), which contribute to the last phase of a muscarinic membrane depolarization (30). In contrast, strong immunoreactivity to the M2 receptor was found in dendrites and somata of interneurons (41) and in neurons of the reticular thalamic nucleus (42). The finding that lemniscal and nonlemniscal MGB express different amounts of M1 and M2 receptors, both immunohistochemically and at the messenger level, is consistent with the heterogeneous pattern of muscarinic receptor distribution found elsewhere in the thalamus (25, 26). Because rat MGB, and MGd in particular, has few (<1%) interneurons (43), we believe our data were mainly derived from sensory relay neurons. Furthermore, the persistence of a postsynaptic muscarinic membrane current under tetrodotoxin and the presence of a high level of M2 receptor mRNA in MGD extracts are consistent with the previous finding that the muscarinic effects result primarily from postsynaptic receptor activation. It is, however, unknown at this time whether similar functional differentiation of muscarinic receptors also exists in nonauditory thalamic nuclei. Further studies are also needed to clarify the role of other neuromodulators such as norepinephrine or 5-hydroxytryptamine (44). Interestingly, when tested in MGB explants, we found no evidence that norepinephrine or 5-hydroxytryptamine differentially affected MGv and MGd cells (45).

Activation of the cholinergic system plays a pivotal role in sensory event detection, attention, and various forms of associative learning and memory (46–50). Our data indicate that ACh may facilitate auditory signal perception through a mechanism of parallel synaptic modulation in the thalamus. In the primary sensory pathway, ACh enhances synaptic signal relay in a global fashion (20). In the nonlemniscal pathway, cholinergic modulation is adaptive to the context of local neuronal activities. In more depolarized neurons, it suppresses synaptic transmission, thereby preventing weak, perhaps "neutral" acoustic stimuli from bombarding the limbic system. In more hyperpolarized cells and in the presence of synchronized corticothalamic and sensory afferents, ACh prompts burst firing. Such event-triggered synaptic bursting may facilitate the induction of long-term synaptic potentiation or recurrent excitation in the lateral amygdala (51) and/or cortical networks (19), roles that cannot be readily fulfilled by random, single spike discharge (17).

We thank Drs. M. S. Steriade, L. P. Renaud, L. Maler, and N. Suga for reading an early version of the manuscript. This work was supported by a Canadian Institutes of Health Research grant (to B.H.). D.M.M. was the recipient of an Ontario Graduate Scholarship.

1. Graybiel, A. M. (1972) *Brain Behav. Evol.* **6,** 363–393.
2. Diamond, I. T. (1983) in *Somatosensory Integration in the Thalamus*, eds. Macchi, G. R., Rustioni, A. & Spreafico, A. (Elsevier, Amsterdam), pp. 251–272.
3. Ahissar, E., Sosnik, R. & Haidarliu, S. (2000) *Nature* **406,** 302–306.
4. Komura, Y., Tamura, R., Uwano, T., Nishijo, H., Kaga, K. & Ono, T. (2001) *Nature* **412,** 546–549.
5. Winer, J. (1992) in *The Mammalian Auditory Pathway*, eds. Webster, D. B., Popper, A. N. & Fay, R. R. (Springer, New York), pp. 222–409.
6. Jones, E. G. (2001) *Trends Neurosci.* **24,** 595–601.
7. LeDoux, J. E. (2000) *Annu. Rev. Neurosci.* **23,** 155–184.
8. Doron, N. N. & Ledoux, J. E. (2000) *J. Comp. Neurol.* **425,** 257–274.
9. Hu, B. (2003) *Exp. Brain Res.* **153,** 543–549.
10. Huang, C. L. & Winer, J. A. (2000) *J. Comp. Neurol.* **427,** 302–331.
11. Kimura, A., Donishi, T., Sakoda, T., Hazama, M. & Tamai, Y. (2003) *Neuroscience* **117,** 1003–1016.
12. Linke, R. & Schwegler, H. (2000) *Cereb. Cortex* **10,** 753–771.
13. Hu, B. (1995) *J. Physiol. (London)* **483,** 167–182.
14. Senatorov, V. V. & Hu, B. (1997) *J. Physiol. (London)* **502,** 387–395.
15. Jahnsen, H. & Llinas, R. (1984) *J. Physiol. (London)* **349,** 205–226.
16. Kim, U. & McCormick, D. A. (1998) *J. Neurosci.* **18,** 9500–9516.
17. Lisman, J. E. (1997) *Trends Neurosci.* **20,** 38–43.
18. Llinas, R. R., Ribary, U., Jeanmonod, D., Kronberg, E. & Mitra, P. P. (1999) *Proc. Natl. Acad. Sci. USA* **96,** 15222–15227.
19. Beierlein, M., Fall, C. P., Rinzel, J. & Yuste, R. (2002) *J. Neurosci.* **22,** 9885–9894.
20. Steriade, M., Jones, E. G. & McCormick, D. (1997) *Thalamus* (Elsevier, Amsterdam).
21. Hu, B., Steriade, M. & Deschenes, M. (1989) *Neuroscience* **31,** 1–12.
22. Hu, B., Senatorov, V. & Mooney, D. (1994) *J. Physiol. (London)* **479,** 217–231.
23. Mooney, D. M., Hu, B. & Senatorov, V. V. (1995) *J. Pharmacol. Exp. Ther.* **275,** 838–844.
24. Whiteside, G. & Munglani, R. (1998) *Brain Res. Brain Res. Protoc.* **3,** 52–53.
25. Carden, W. B. & Bickford, M. E. (1999) *Neurosci. Lett.* **276,** 153–156.
26. Oda, S., Kuroda, M., Kakuta, S. & Kishi, K. (2001) *Brain Res.* **894,** 109–120.
27. McCormick, D. A. & Feeser, H. R. (1990) *Neuroscience* **39,** 103–113.
28. McCormick, D. A. & Prince, D. A. (1987) *J. Physiol. (London)* **392,** 147–165.
29. Castro-Alamancos, M. A. (2002) *J. Physiol. (London)* **539,** 567–578.
30. Zhu, J. & Heggelund, P. (2001) *J. Neurosci.* **21,** 1148–1159.
31. Weyand, T. G., Boudreaux, M. & Guido, W. (2001) *J. Neurophysiol.* **85,** 1107–1118.
32. Steriade, M. (2001) *Nat. Neurosci.* **4,** 671.
33. He, J. & Hu, B. (2002) *J. Neurophysiol.* **88,** 2152–2156.
34. McQuiston, A. R. & Madison, D. V. (1999) *J. Neurosci.* **19,** 5693–5702.
35. Shen, K. Z. & North, R. A. (1992) *J. Physiol. (London)* **455,** 471–485.
36. McCormick, D. A. & Prince, D. A. (1986) *Nature* **319,** 402–405.
37. McCormick, D. A. & Pape, H. C. (1988) *Nature* **334,** 246–248.
38. Buller, A. L., Larson, H. C., Schneider, B. E., Beaton, J. A., Morrisett, R. A. & Monaghan, D. T. (1994) *J. Neurosci.* **14,** 5471–5484.
39. Gonzalez-Lima, F. & Cada, A. (1994) *Neuroscience* **63,** 559–578.
40. Wall, S. J., Yasuda, R. P., Hory, F., Flagg, S., Martin, B. M., Ginns, E. I. & Wolfe, B. B. (1991) *Mol. Pharmacol.* **39,** 643–649.
41. Plummer, K. L., Manning, K. A., Levey, A. I., Rees, H. D. & Uhlrich, D. J. (1999) *J. Comp. Neurol.* **404,** 408–425.
42. Carden, W. B. & Bickford, M. E. (1999) *J. Comp. Neurol.* **410,** 431–443.
43. Winer, J. A. & Larue, D. T. (1996) *Proc. Natl. Acad. Sci. USA* **93,** 3083–3087.
44. McCormick, D. A. (1993) *Prog. Brain Res.* **98,** 303–308.
45. Mooney, D. M. (2001) Ph.D. thesis (Univ. of Ottawa, Ottawa).
46. Sanford, L. D., Silvestri, A. J., Ross, R. J. & Morrison, A. R. (2001) *Arch. Ital. Biol.* **139,** 169–183.
47. Silvestri, A. J. & Kapp, B. S. (1998) *Behav. Neurosci.* **112,** 571–588.
48. Suga, N., Gao, E., Zhang, Y., Ma, X. & Olsen, J. F. (2000) *Proc. Natl. Acad. Sci. USA* **97,** 11807–11814.
49. Weinberger, N. M. & Bakin, J. S. (1998) *Audiol. Neurootol.* **3,** 145–167.
50. Perry, E., Walker, M., Grace, J. & Perry, R. (1999) *Trends Neurosci.* **22,** 273–280.
51. Clugnet, M. C. & LeDoux, J. E. (1990) *J. Neurosci.* **10,** 2818–2824.